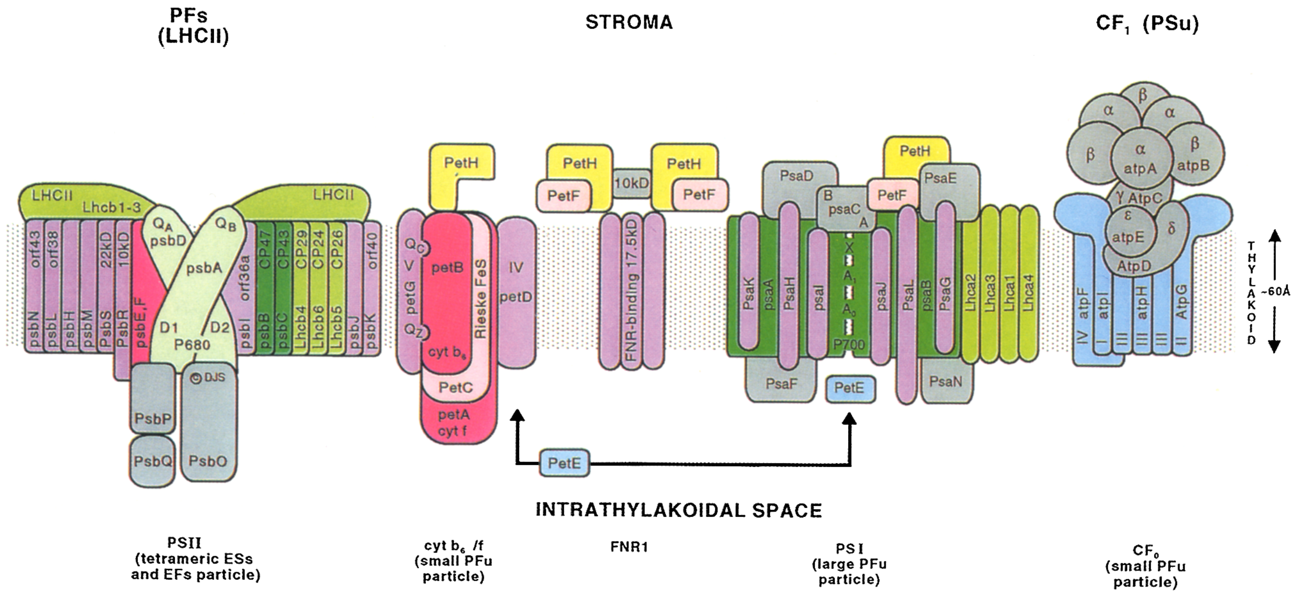

I Schematic arrangement of polypeptides that have been identified as components of barley thylakoid membranes from freeze-fracture electron microscopy, gel electrophoresis, and biochemical studies. CF_0 and CF_1, coupling factors; EFs, endoplasmic fracture face; ESs, endoplasmic surface; and PFs, protoplasmic fracture face of stacked thylakoids. PFu, protoplasmic fracture face, and PSu, protoplasmic surface of unstacked thylakoids. Many PSII polypeptides are named after the genes coding them. (Courtesy: D.J. Simpson, Carlsberg Laboratory, Copenhagen.)

A colour version of these plates is available for download from www.cambridge.org/9780521644976

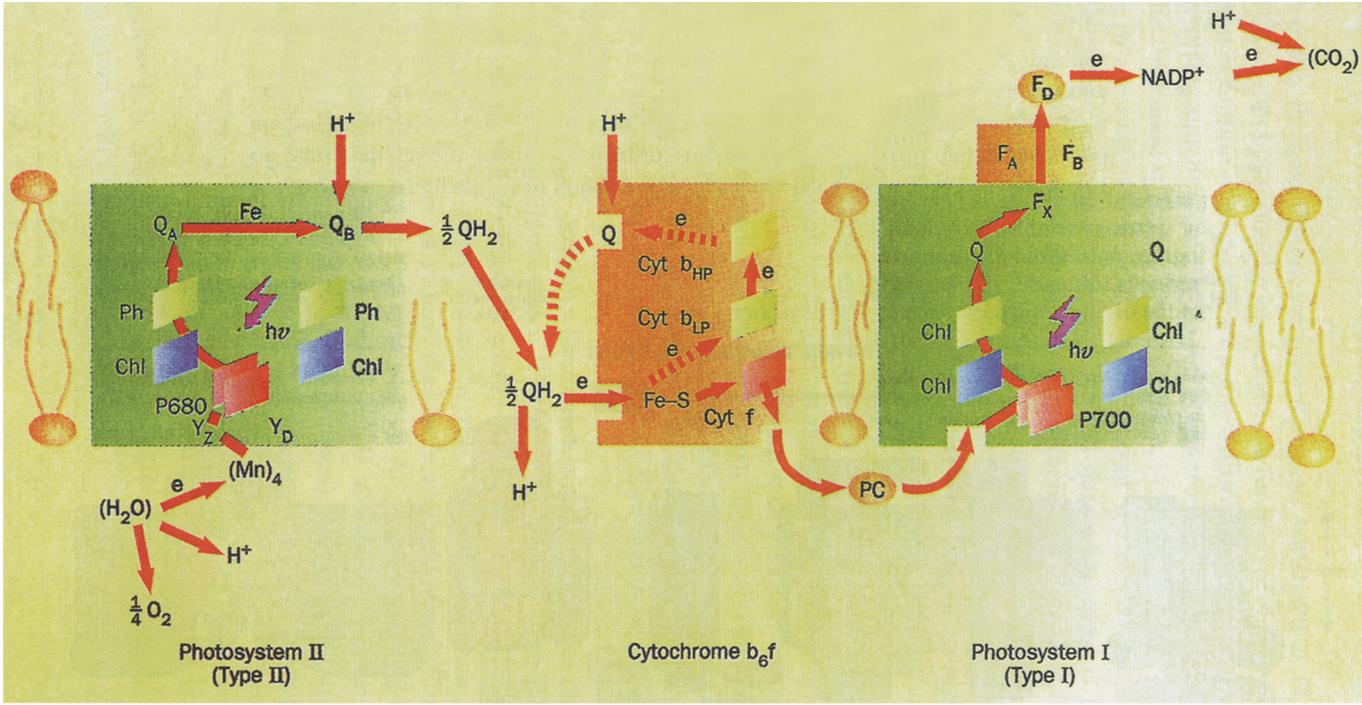

II Schematic depiction of the three thylakoid membrane complexes (PSII, cytochrome $b_6 f$ and PSI) and the mobile carriers (quinone, plastocyanin and ferredoxin) which function in photosynthetic water oxidation, electron (and proton) transport and CO_2 reduction in chloroplasts. (Courtesy: J. Barber, Imperial College, London.)

III Chloroplasts in the guard cells of *Phyllitis scolopendrium*, a fern. (Courtesy: T. A. Mansfield, Lancaster University, UK.)

(a)

(b)

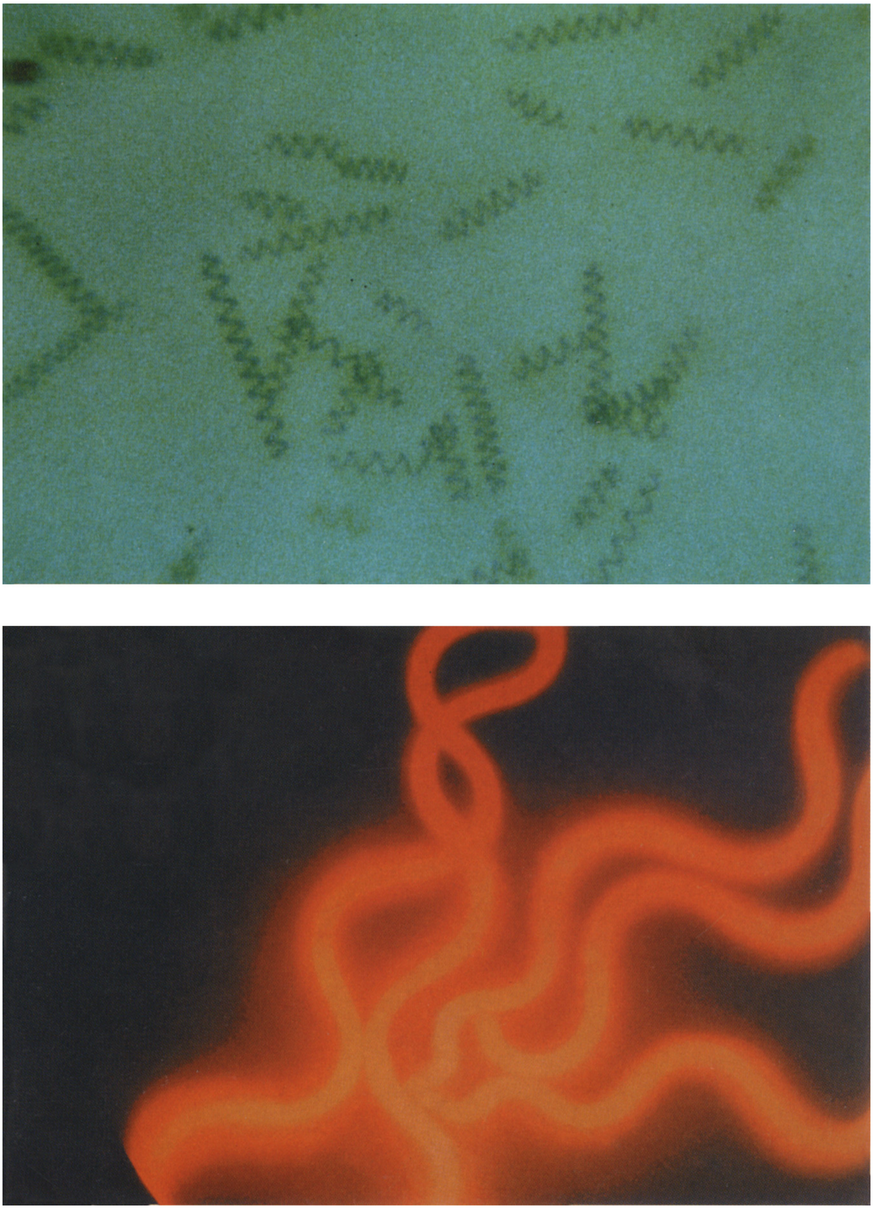

IV (**a**) Cells of the cyanobacterium *Spirulina platensis.* (**b**) *S. platensis* fluorescing in light. (Courtesy: A. Vonshak, Ben Gurion University, Israel.)

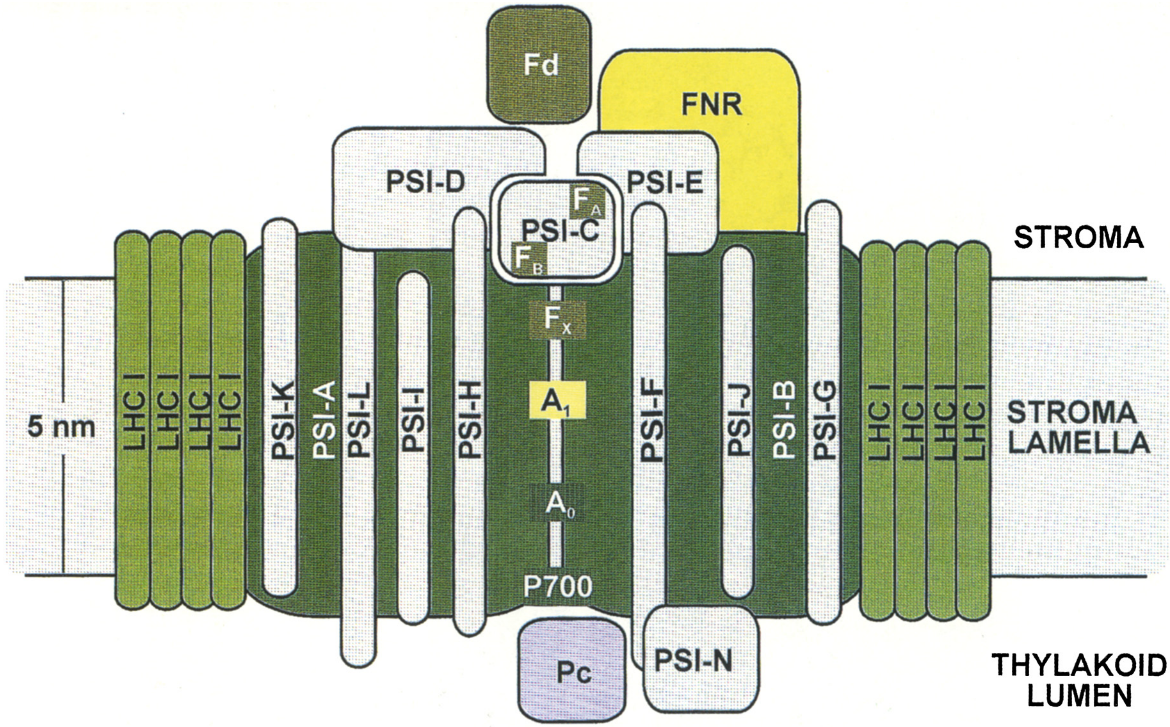

V Schematic representation of the PSI complex in higher plants (Source: Scheller, Naver and Møller, 1997). (See also §8.9.)

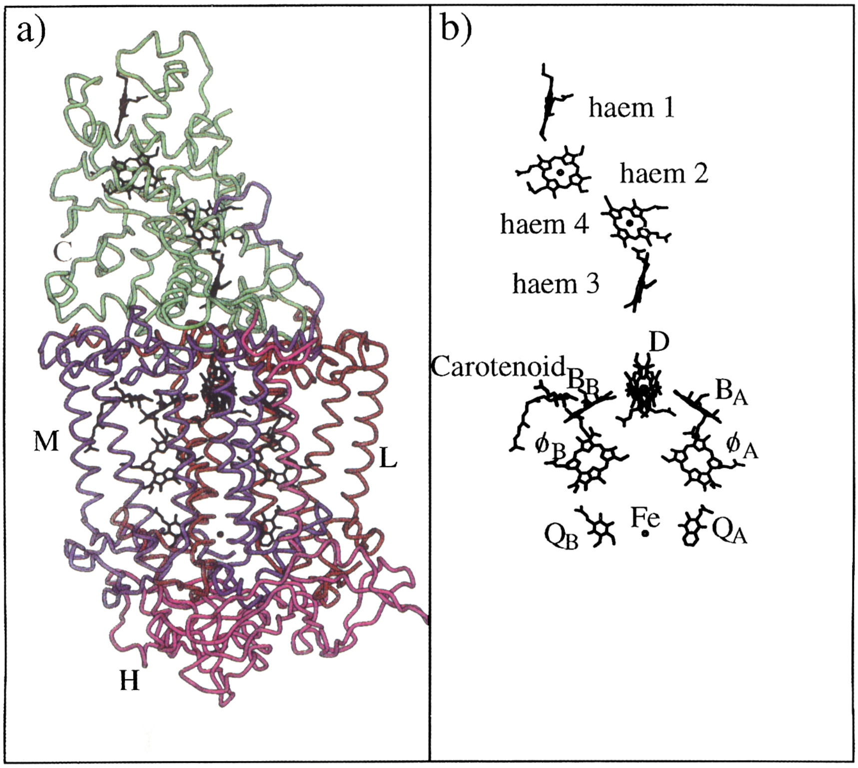

VI The structure of the photosynthetic reaction centre from *Rhodopseudomonas viridis.* (**a**) The four polypeptide subunits of the reaction centre are displayed as C_α traces and are colour coded as: C subunit, green; L, brown; M, blue; and H, purple. The cofactors are displayed in black. (**b**) The 14 cofactors of the reaction centre. The four haems are covalently bound by the C subunit; the other 10 factors are non-covalently bound by the L and M subunits. D, BChl *b* dimer; B_A and B_B, monomeric BChl *b*; ϕ_A and ϕ_B, BPheo *b*; Q_A, menaquinone; Q_B, ubiquinone; Fe, non-haem iron. The carotenoid is 1,2-dihydroneurosporene. The figure has been generated with the MolScript computer program (Kraulis P.J. (1991). *J. Appl. Cryst.* 24, 946–50), reference: C.R.D. Lancaster and H. Michel (1996). (Courtesy: H. Michel and C.R.D. Lancaster, Max-Planck Institute for Biophysics, Frankfurt, Germany.)

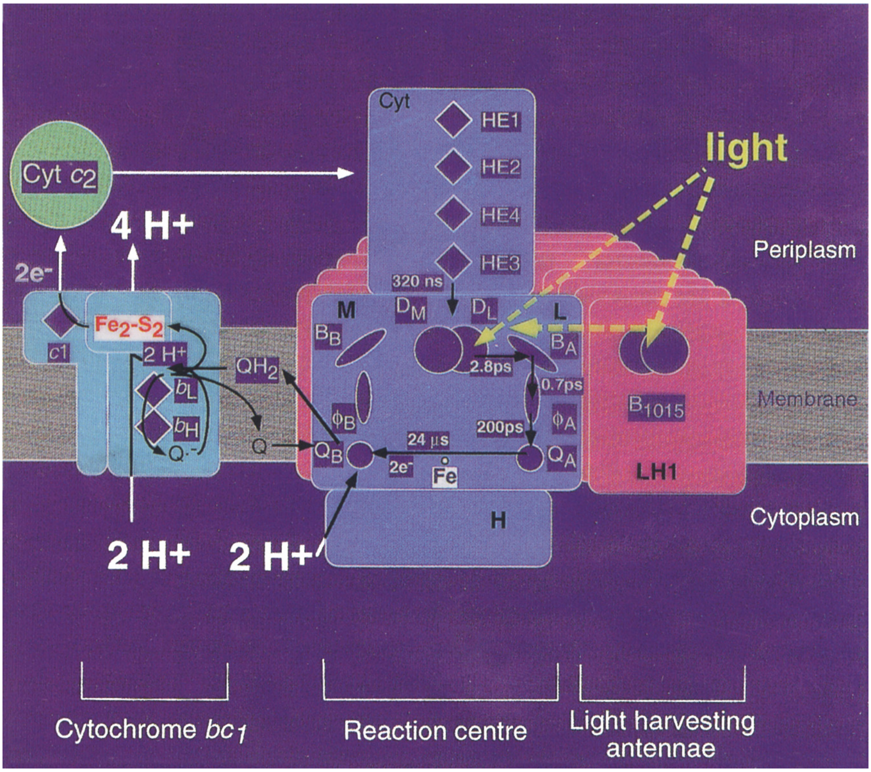

VII Light-driven electron transfer in *Rhodopseudomonas viridis*. HE, haem. For other symbols, refer to Plate VI and to Lancaster and Michel (1996). (Courtesy: C.R.D. Lancaster and H. Michel, Frankfurt, Germany.)

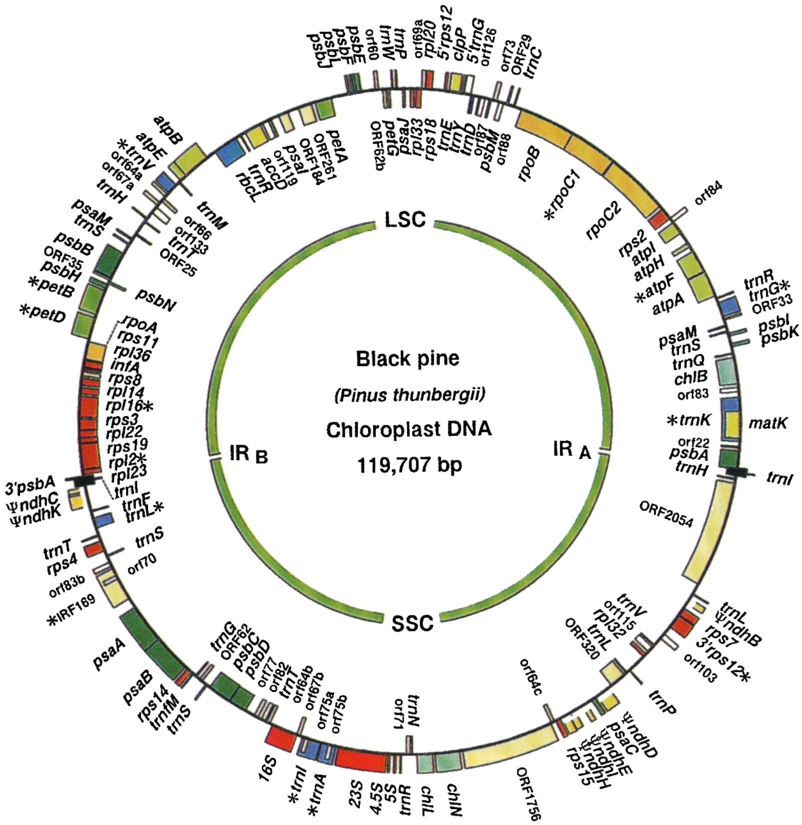

VIII Genetic map of the black pine *Pinus thunbergii* chloroplast DNA. See Fig. 8.1 for gene arrangements and explanation of symbols. Details in Wakasugi *et al.* (1994). (Courtesy: M. Sugiuro, Nagoya University, Japan.)

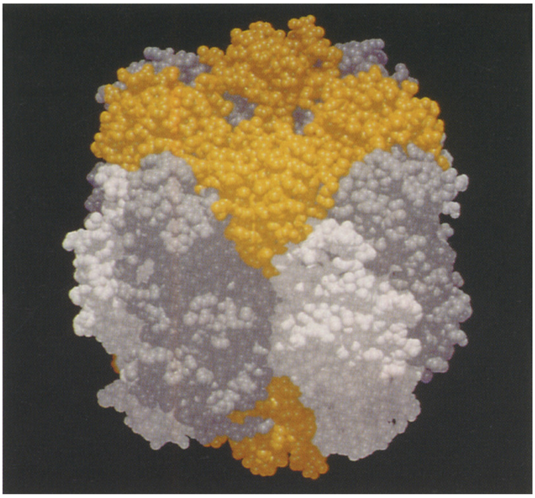

IX High-resolution X-ray crystallographic structure of spinach RuBisCO. **Top**. The L_8S_8 hexadecamer. The eight large (L) subunits (475 residues, *c.* 55 000 kDa) are shown in two shades of grey and the eight small (S) subunits (123 residues, *c.* 15 000 kDa) are shown in yellow. The L_8S_8 hexadecamer can be regarded as a tetramer of L_2S_2 units (see *bottom*) around a fourfold symmetry axis. **Bottom**. The L_2S_2 unit. The two active sites with bound transition state analogue, 2-carboxyarabinitol-bisphosphate (in red) are located at the interface of the L subunits in the L_2 dimer. For details refer to I. Andersson (1996). (Courtesy: I. Andersson, Swedish University of Agricultural Sciences, Uppsala, Sweden.)

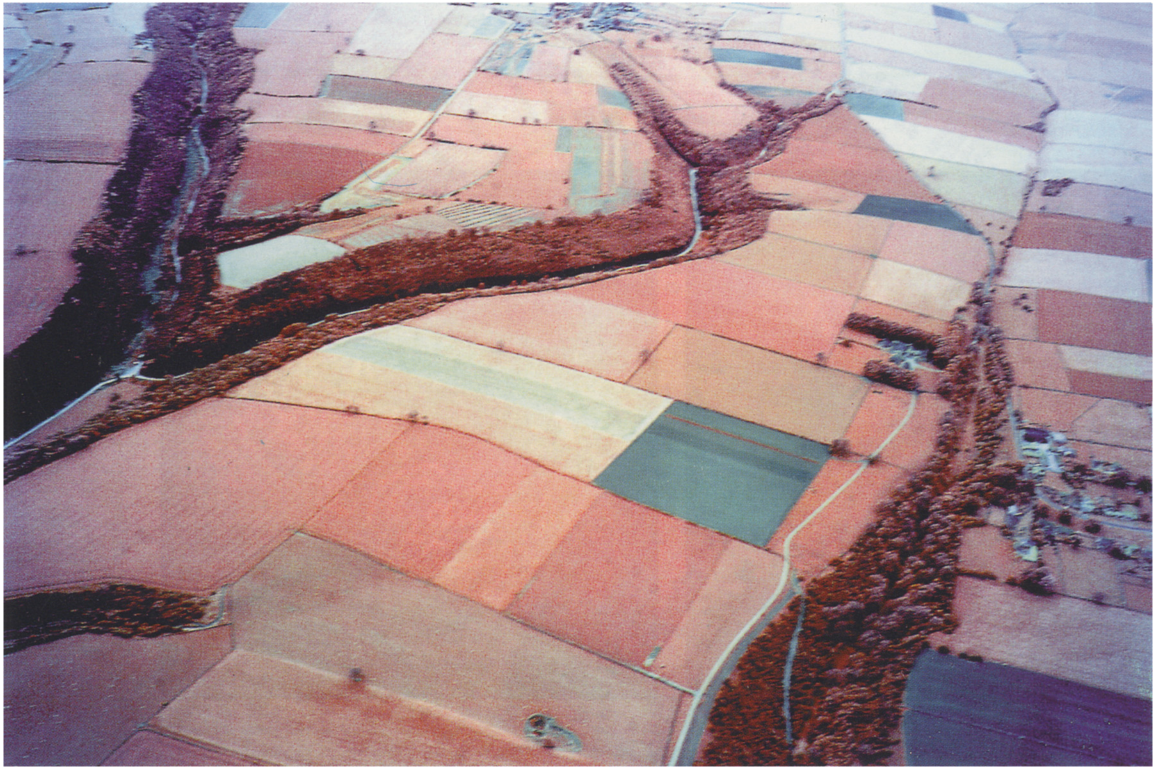

X Aerial colour infra-red photograph of farmland taken with a Kodak Science™ 420 CIR digital camera. Different vegetation types show as varying shades of red and the bare soil in green. (Courtesy: Geotechnologies, Bath, UK.) (See House *et al.*, 1999.)

XI Measurement of photosynthesis in the field using the Hansatech FMS_2 Pulse Modulated Chlorophyll Fluorimeter. This portable fluorimeter contains all the light sources and electronics necessary for measurement of chlorophyll fluorescence during photosynthesis under natural light in field conditions. (Courtesy: Hansatech Instruments Ltd, Pentney, Norfolk, UK.)

XII Advanced Portable LCA-4 IRGA for photosynthesis and transpiration measurements. (Courtesy: ADC Bioscientific Ltd, Hoddesdon, UK.)

XIII The ADC 2250 for measurements of gas exchanges on the infra-red absorption principle. The high-performance Omega optical bench provides simultaneous absolute and differential gas measurements. (Courtesy: ADC Bioscientific Ltd, Hoddesdon, UK.)

XIV Portable leaf area meter for measurements of areas of leaves in the field and laboratory. (Courtesy: LI-COR Inc., Lincoln, Nebraska, USA.)

XV The LI-6400 Portable Photosynthesis System for measurement of canopy of CO_2 gas exchange and instantaneous estimation of light conversion efficiency.
(Courtesy: LI-COR Inc., Lincoln, Nebraska, USA.)

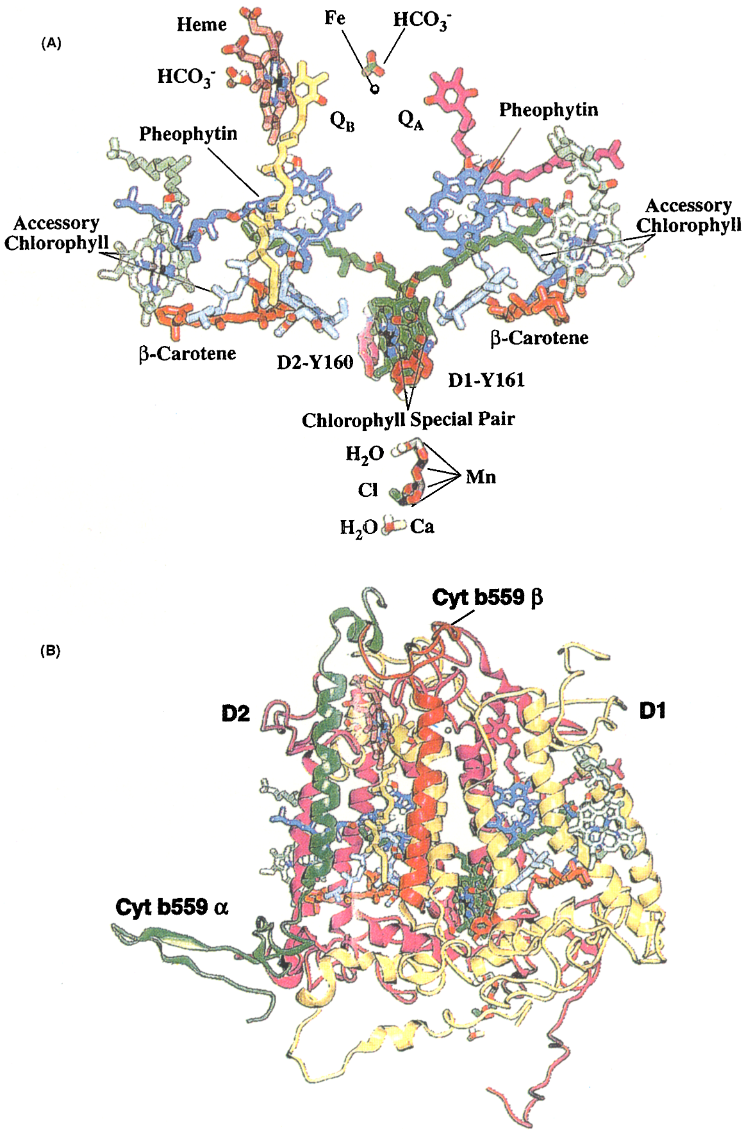

XVI (A) The modelled components in the PSII reaction centre of the green alga *Chlamydomonas rheinhardtii.* (B) The combination of D_1/D_2 and cytochrome *b*559 (in α/β form) proteins and the bound cofactors in the reaction centre. (From Xiong *et al.* Photosynthesis Research 1998. Courtesy: Govindjee.)